Theoret. Chim. Acta (Berl.) 62, 195–207 (1983)

THEORETICA CHIMICA ACTA

Original Investigations

Application of an Economical Method for the Calculation of Molecular Correlation Energies to the Study of a Potential Energy Surface: The HO_2 Radical Dissociation Process

Jean-Yves Metz* and Jacques Lievin

Laboratoire de Chimie Physique Moléculaire, Faculté des Sciences, CP. 160, Université Libre de Bruxelles, B-1050 Bruxelles, Belgique

A simplified method for the calculation of molecular correlation energies, developed previously, is applied to the study of the potential energy hypersurface related to the reaction $O_2 + H \rightarrow HO_2 \rightarrow OH + O$. The main parameters that characterize the topology of the surface have been determined: the equilibrium geometries and vibrational frequencies of HO_2 and of its dissociation products, the dissociation energies, the energy gap between the dissociation limits, the geometry of an activated complex, and the corresponding potential barrier height. The particular importance of including the correlation energy is discussed for each of the calculated parameters. In spite of the minimal computational effort required, the results are in good agreement with the experimental data on the one hand, and with the results proceeding from elaborate variational calculations on the other hand. Moreover the controverted existence of a potential barrier (0.19 eV) along the $O_2 + H \rightarrow HO_2$ recombination path is discussed.

Key words: Hydroperoxyl radical-Potential energy surface–Molecular correlation energy.

1. Introduction

The reaction:

$$H(^2S) + O_2(^3\Sigma_g^-) \rightarrow HO_2(^2A'') \rightarrow OH(^2\Pi) + O(^3P)$$

---

* Boursier I.R.S.I.A.

plays an important role in combustion studies [1] and in atmospheric chemistry [2] since it produces the particularly reactive radical OH.

The intermediate species HO_2 has been the object of several theoretical studies around its ground state equilibrium geometry [3] but, to our knowledge, only three studies [4] have been devoted to the calculation of the potential energy surface relative to the reaction mentioned above. One of the most outstanding points of these studies is the controversy concerning the eventual existence of an activation barrier along the $H+O_2$ recombination path.

The purpose of this work is not to calculate a complete correlated potential surface, but rather to test the ability of reproducing the main features of this surface by using an economical method for molecular correlation energy calculations developed previously [5, 6, 7]. In this context, we will be interested to compute accurately equilibrium geometries and vibrational frequencies of the intermediate radical on the one hand and of its dissociation products on the other hand. Geometries of the activated complex, dissociation and activation energies will also receive particular attention. Such a method could be of great interest in view of computing economically whole potential energy surfaces to be used in classical trajectory computations.

2. Methods of Calculation

2.1. Zeroth-Order Wavefunction

The first requirement of the method used here is to define a zeroth-order wavefunction which ensures a proper description of the correct Wigner–Witmer dissociation fragments. This function may be constructed from the data of Table 1, where the orbitals of HO_2 are correlated to those of the dissociation products. The axes convention adopted for HO_2 is presented in Fig. 1.

Table 1. Correlation between HO_2 and its dissociation products

HO_2	$1a'$	$2a'$	$3a'$	$4a'$	$5a'$	$6a'$	$7a'$	$8a'$	$1a''$	$2a''$
O_2+H	$1\sigma_g$	$1\sigma_u$	$2\sigma_g$	$2\sigma_u$	$3\sigma_g$	$1\pi_u$	$1\pi_g$	$1s$	$1\pi_u$	$1\pi_g$
$OH+O$	1σ	$1s$	2σ	$2s$	3σ	$2p_y$	$2p_z$	1π	1π	$2p_\alpha$

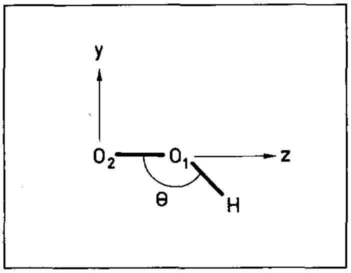

Fig. 1. Axis convention for HO_2

It can first be shown that the SCF configuration of HO_2:

Conf. (A): $(1\text{–}6)a'^2 1a''^2 7a'^2 2a''$

gives rise to the improper ionic products $O_2^- + H^+$ and $OH^+ + O^-$. It is thus necessary to form a multiconfigurational zeroth-order wavefunction which combines Conf. (*A*) with the configurations corresponding to the proper dissociation limits $O_2 + H$ and $OH + O$. These configurations can directly be deduced from the ground state SCF configurations of the dissociation products (C_s symmetry group):

Conf. ($O_2(^3\Sigma_g^-)$): $1\sigma_g^2 1\sigma_u^2 2\sigma_g^2 2\sigma_u^2 3\sigma_g^2 1\pi_u^4 1\pi_g(a')1\pi_g(a'')$

Conf. ($H(^2S)$): $1s(a')$

Conf. ($OH(^2\Pi)$): $1\sigma^2 2\sigma^2 3\sigma^2 1\pi^2(a'')1\pi(a')$

Conf. ($O(^3P)$: $1s^2 2s^2 2p^2(a')2p(a')2p(a'')$

The result is that the same configuration:

Conf. (B): $(1\text{–}6)a'^2 1a''^2 7a'8a'2a''$

describes both dissociation channels.

Moreover, as in the case of the dissociation of OH [8] and HCN [7] the addition of a third configuration:

Conf. (C): $(1\text{–}6)a'^2 1a''^2 8a'^2 2a''$

should improve the description of the zeroth-order wavefunction at intermediate internuclear separations by ensuring a smooth change from Conf. (A) to Conf. (B) along the dissociation coordinate. It is important to note here that the use of a deficient configuration expansion in these intermediate regions can produce artificial potential energy barriers that could be falsely interpreted as activation barriers. Figure 2 illustrates the variation of the relative contributions to the

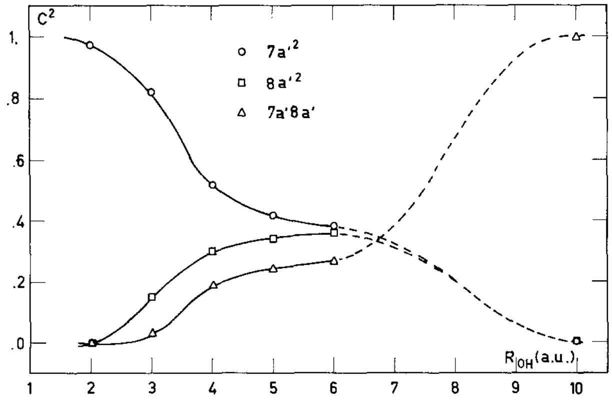

Fig. 2. Square modulus of the MCSCF coefficients of the zeroth-order wavefunction (basis set STO-3G) as a function of the R_{OH} dissociative coordinate. Cross section in the potential surface with $R_{OO} = 2.21$ a.u. and $\Theta = 104°$

zeroth-order wavefunction of the three configurations in a cross-section of the potential hypersurface along the OH dissociation coordinate.

2.2. Correlation Energy Calculations

The simplified method for the molecular correlation energy calculations used in this work has been developed elsewhere [7]. It is inspired from the partitioning of Sinanoglu et al [9, 10] who define different types of excitations with respect to a particular subspace (the "Hartree–Fock sea") shown equivalent to the "valence orbital space" in a molecular context defined in the complete orbital space. These excitations generated from the zeroth-order wavefunction are limited to the first order of perturbation (i.e. the biexcitations). The three types of contributions are:

(1) the internal correlation energy corresponding to biexcitations within the valence space.
(2) the semi-internal correlation energy represented by one excitation within and the other outside the valence space
(3) the all-external correlation energy corresponding to pair excitations outside the valence space.

In this context, we have proposed earlier to evaluate the correlation energy by performing two separate calculations: the first for the *internal* correlation energy (E^{I}_{CORR}) and the second one for the *non-internal* correlation energy (E^{NI}_{CORR}) which regroups the semi-internal and all-external contributions. The internal part will be treated variationally while the non-internal part will be evaluated by a semi-empirical "atoms-in-molecule" method. This choice can be justified by the fact that if variational calculations can be achieved for the internal correlation, it is not true for the non-internal part as a consequence of the necessary limitations imposed to the size of the configurational and basis set spaces.

2.2.1 Internal Correlation Energy. MCSCF calculations performed with the complete internal configuration space become rapidly out of hand when the molecular size increases. That is why the validity of an alternative two step MC_n (ext)/CI(ext) procedure[1] has been tested [7]. The total energies obtained in this way converge rapidly with the number of configurations n included in the first step (MCSCF calculation). In fact the rapidity of this convergence allows one to conclude that a satisfactory approximation is to limit the MCSCF expansion to the zeroth-order wavefunction; the remaining internal correlation energy is then evaluated in the second step (CI calculation).

A second approximation to the above procedure consists in substituting a minimal basis set to the extended set for the CI calculation; this approximation was also extensively tested previously [7] and shown to give reliable results.

---

[1] This procedure consists in performing in a first step an MCSCF calculation with a configurational space limited to n components and in a second step a CI calculation on the complete internal space with the optimized orbitals arising from the first step. The "ext" notation specifies that the same extended basis set has been used at the two levels of the procedure.

It is this latter method that is used in the present calculations, and thus the two-step procedure will henceforth be denoted MC_0(ext)/CI(min).

2.2.2. Non-internal Correlation Energy. The basic idea of the "atoms-in-molecule" method is to express the molecular non-internal correlation energy as a weighted sum of atomic non-internal correlation energies which are known semi-empirically through Hartree-Fock-Dirac calculations [11] performed on a set of atomic and ionic configurations. Two distinct approaches have been developed to operate the decomposition of the molecular structure:

(1) a population analysis approach [5,6]
(2) a LCAO expansion approach [7].

The second one is well adapted to the present study which requires as mentioned above the use of a multiconfigurational zeroth-order wavefunction. This approach consists in an expansion of this function into a linear combination of atomic determinants using the LCAO and MCSCF coefficients to derive the expansion coefficients. Each atomic determinant corresponding to a neutral or ionic configuration of a constituting atom A may be expanded in terms of LS eigenfunctions $\{\Gamma(A)\}$ arising from the considered configuration of this atom. It may be shown that the molecular non-internal correlation energy is then given by:

$$E^{NI}_{\mathrm{CORR}}\ (\mathrm{MOL}) = \frac{\sum_i b_i^2 \sum_A E^{NI}_{\mathrm{CORR}}\ (\Gamma^i(A))}{\sum_i b_i^2}$$

where the normalization factor is imposed by the neglect of coupling between the atomic determinants.

2.3. Comparison wtih Other Theoretical Work

Table 2 gives a summary of the main features of the present calculations as well as those of other work on this system. It appears from these data that the method used here requires minimal computational efforts as compared to the other elaborate calculations.

Table 2. Comparison of theoretical methods

Reference	Basis set	Size of MCSCF space[a]	Size of CI reference space[a]	Size of CI space[a]
L.J. [4]	$(4s2p1d\|3s1p)$	/	30	10 000[b,c]
M.B. [4]	$(4s2p1d\|2s1p)$	20	54	2 292[b]
D.W.G. [4]	$(3s3p1d\|2s1p)$	/	30	322[d]
		/	30	11 670[e]
This work	$(3s2p1d\|2s1p)$	3	/	/
	$(2s1p\|1s)$	3	3	120

[a] Number of CSF'S.
[b] Mono- and biexcitations with respect to the reference space.
[c] Dimension of the resulting hamiltonian matrices.
[d] GVB-CI calculation.
[e] POL-CI calculation.

2.4. Computer Programs

1. The MCSCF program ALIS written by Ruedenberg et al. [12]
2. The CI program of Whitten et al. [13]
2. The non-internal correlation energy program written by J. Breulet.

2.5. Basis Sets

Two well-known basis sets are used:

1. the double zeta plus polarization 6–31G** basis set [14]
2. the minimal STO-3G basis set [15].

3. Results and Discussion

3.1. Basis Set Improvements

As a starting point to this study we have tested the adequacy of the 6-31G** basis set scale factors to reproduce at the zeroth-order level of calculation (refered to as MC_0(6–31G**)) correct energy differences between the two dissociation channels on the one hand and between HO_2 and these channels on the other hand. Preliminary tests showed that the scale factor corresponding to the outer part of the sp shell of the oxygen atoms had to be considered only because of its high sensitivity to the chemical neighbourhood. The standard value proposed in the literature [16] for this scale factor is 0.98, which was established by optimization on the CH_2O and H_2O systems. This value is in fact too large for the OH radical (optimal value: 0.97) and too small for O_2, O and HO_2 (optimal values: 1.00, 0.99 and 0.99 respectively)[2]. Several tests have shown that an adjustment of this scale factor to a value of 1.03 gives a better balance in the energies of the different partners. This improvement can be illustrated by the following comparison relative to the energy difference ΔE between the two dissociation limits O_2+H and $OH+O$:

$$\Delta E(B1) = -1.86\,\text{eV}$$
$$\Delta E(B2) = -1.58\,\text{eV}$$
$$\Delta E(\text{HF}) = -1.58\,\text{eV}$$

where $B1$ and $B2$ refer respectively to the standard and modified scale factor of the 6-31G** basis set, and HF to the result obtained by using estimated Hartree–Fock energies[3] (see Ref. 17, 18 and 19 for O_2, OH and O). It can be pointed out however that these near Hartree–Fock results are in complete disagreement with the experimental value $\Delta E = +0.6$ eV. The reason for that is obviously the lack of correlation energy. The same comparison is unfortunately impossible for the energy of HO_2 for which no "Hartree–Fock" energy is available in the literature. However the use of the modified basis set instead of

---

[2] The optimal values were obtained using SCF calculations.

[3] The MC_0 energies of the dissociation limits can be compared to H.F. energies as a consequence of the definition of the zeroth-order wavefunction (see Section 2.1).

the standard one does not affect the energy of HO_2 at its equilibrium geometry to a large extent (~ 0.1 eV).

3.2. Equilibrium Geometries and Vibrational Frequencies

The calculated results obtained for the parameters which characterize the potential energy surface in the vicinity of the HO_2 equilibrium geometry and of the two dissociation limits are collected in Table 3. Three levels of approximation are considered:

(1) MC_0(6-31G**): zeroth-order wavefunction calculation
(2) MC_0(6-31G**)/CI(STO-3G): inclusion of the internal correlation energy
(3) MC_0(6-31G**)/CI(STO-3G)+NI: inclusion of the non-internal correlation energy leading to total energies.

The equilibrium geometries and vibrational frequencies given in Table 3 have been derived from a quadratic expression of the potential energy. For HO_2, coupling terms have been introduced in the analytical function. It must be pointed out that the lack of anharmonic terms gives the well-known result that the vibrational frequencies are over-estimated. Pulay et al. [20] have shown that empirical corrections performed on the diagonal force constants (10% for stretching modes and 20% for bending modes) give a reasonable order of magnitude for these anharmonicity corrections. Calculated frequencies taking these corrections into account are given in parentheses in Table 3. Furthermore, it is important to note that the very simple model used here to fit the potential function may be sensitive to the choice of the calculated points around the minimum. On the basis of earlier tests [7], we estimate the numerical accuracy of the fitting to be about 100 cm^{-1}. It appears from Table 3 that the incidence of the inclusion of correlation energy on the results is quite different for HO_2 than for the dissociation fragments. Mainly the addition of internal correlation gives rise to the following effects:

(1) a large increase (~0.1 a.u.) of the bond lengths for O_2 and OH, but only a slight change (<0.03 a.u.) for HO_2
(2) a decrease of the vibration frequencies for O_2 and OH and a large increase for HO_2

These differences can be explained by the fact that the zeroth-order wavefunction has been constructed (see section 2.1) to ensure proper dissociation of HO_2 into O_2+H and $OH+O$ but not to describe the processes $O_2 \rightarrow 2O$ or $OH \rightarrow O+H$. It follows that the MC_0 calculations performed on O_2 and OH correspond in fact to purely SCF calculations leading to improper ionic dissociation limits for these species and therefore the well-known shortcomings of this level of approximation are observed, i.e. too short equilibrium distances and too large frequencies. The addition of the CI contributions to the MC_0 curves stabilizes more significantly the dissociation limits than the minima of the curves: indeed these contributions not only include the internal correlation energy of O_2 and OH but also, at large distances, correct their dissociation limits to proper neutral products.

Table 3. Equilibrium geometries and vibrational frequencies for HO_2, O_2 and OH

System	Property[a]	MC_0	MC_0/CI	MC_0/CI+NI[b]	L.J.[c]	M.B.[c]	D.W.G.[c] POL-CI	D.W.G.[c] GVB-CI	Exp.
OH	R_e	1.81	1.89	1.87	—	1.85	—	—	1.83 [21]
	ω_e	3530	3351	3280	—	—	—	—	3735 [23]
O_2	R_e	2.21	2.33	2.33	—	2.33	2.33	2.31	2.28 [21]
	ω_e	1817	1771	1757 (1667)	—	—	—	—	1580 [21]
HO_2	R_{OO}	2.49	2.46	2.46	2.53	2.58	2.59	2.58	2.49 [22]
	R_{OH}	1.85	1.87	1.87	1.84	1.88	1.87	1.86	1.83 [22]
	Θ	105	105	104	104.2	104.2	103.3	103.3	104 [23]
	ω_1	2663	4667	4060 (3854)	3905	—	3655	3612	3414 [23]
	ω_2	1049	1456	1518 (1380)	1478	—	1436	1438	1389 [23]
	ω_3	853	1124	1292 (1177)	1125	—	1181	1110	1011 [23]

[a] Distances in a.u., angle in degrees and frequencies in cm^{-1}.

[b] Results in parentheses refer to corrected values for anharmonicity effects.

[c] See Table 2 for a description of these calculations.

As a consequence an important flattening of the potential curves is observed with a corresponding decrease of the calculated frequencies and an increase of the distances.

For HO_2 a quite different situation occurs because the potential surface is already flattened at the MC_0 level of calculation. Therefore the inclusion of the CI increments contributes only to internal correlation with larger energy contributions at the shorter internuclear distances than at the larger ones. This explains the large increase observed in the calculated frequencies. The small changes observed for the equilibrium distances can be attributed to the presence of a maximum in the CI energy contribution near the minimum of the MC_0 potential surface.

We note, moreover, that the HOO angle value seems to be independent of the correlation effects.

Comparison of our calculated results with the corresponding experimental data shows that the equilibrium geometries agree quite well, with discrepancies of about 0.04 a.u. for the distances and 1° for the HOO angle. The agreement is not so good for the frequencies for which we register an over-estimate of about 10% for the values corrected for anharmonicity deformations. However, in view of the simple model used here, this agreement may be considered as satisfactory.

On the whole our results are also in agreement with those proceeding from other theoretical work (see Section 2.3).

3.3. Energy Differences

We report in Table 4 the calculated dissociation energies of HO_2 and the energy difference ΔE between the two dissociation channels together with the corresponding results found in the literature. The effect of the progressive inclusion of correlation energy on the calculated energies is particularly spectacular. This evolution is illustrated in Fig. 3. It can be seen that a factor of two is observed between the MC_0 and MC_0/CI results for the dissociation energies and that the sign of the ΔE value changes with the inclusion of the internal correlation energy. The results calculated at the MC_0/CI+NI level are found to be in good agreement with the corresponding experimental values with discrepancies of

Table 4. Energy differences[a] (in eV)

Process	MC_0	MC_0/CI	MC_0/CI+NI	MB[b]	D.W.G.[b] POL-CI	GVB-CI	exp.[c]
$HO_2 \rightarrow OH+O$	0.98	1.97	2.22	2.58	—	—	2.88±0.09
$HO_2 \rightarrow O_2+H$	2.56	1.38	1.79	2.2	1.83	1.74	2.24±0.09
$O_2+H \rightarrow OH+O$	−1.58	0.59	0.43	0.38	—	—	0.62

[a] D_e values.

[b] Other work calculated results; see Table 2 for a description of these calculations.

[c] Values calculated by means of thermochemical cycle[23] and corrected for zero point energies [23]

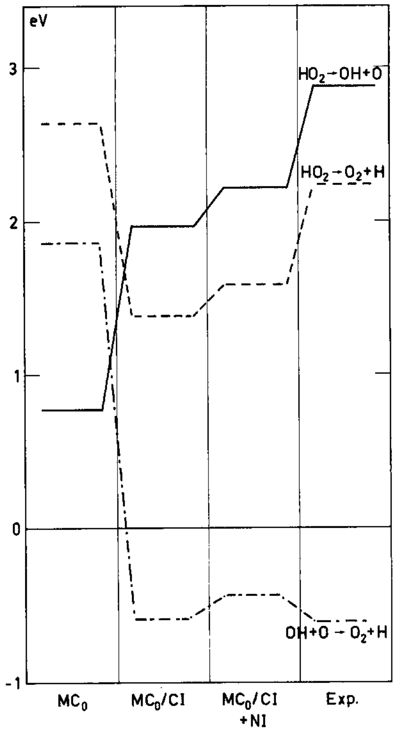

Fig. 3. Evolution of the dissociation energies relative to the dissociation channels O_2+H and $OH+O$ and the energy difference between these channels as a function of the progressive inclusion of correlation energy

$\sim$25%, which is the same order of accuracy as that previously observed [7] for similar systems. Also, our results agree with the values of D.W.G. for the $H—O_2$ bond energy and with the value of M.B. for ΔE. However, the elaborate calculations of M.B. give superior results for both dissociation energies.

3.4. *Incoming Channel* $H+O_2 \rightarrow HO_2$

In this section, we present exploratory calculations performed along the $H+O_2 \rightarrow HO_2$ channel to discuss the presence of a potential barrier along this path. Previous calculations of both M.B. and D.W.G. predict the existence of such a barrier, although those of L.J. contest this feature. We localized the top of the barrier in two steps. In a first step, a cross section through the potential surface was performed with fixed values for Θ an R_{OO} in order to determine the R_{OH} distance corresponding to the maximum of the barrier. The fixed values for Θ and R_{OO} are the equilibrium values in HO_2 and O_2 respectively, i.e. $\Theta = 104°$ and $R_{OO} = 2.212$ a.u. The curves that result from this cross section at the three characteristic levels of approximation are shown in Fig. 4. It appears that a quite small potential barrier ($\sim$0.06 eV)[4] is encountered at the MC_0 level of calculation. A more consequent barrier ($\sim$.47 eV)[4] is induced by the inclusion of internal correlation energy and the non-internal correlation reduces its height to $\sim$0.35 eV.[4]

---

[4] These values correspond to the energy difference between the maximum of the potential curve along the considered cross section and the products at their equilibrium geometry.

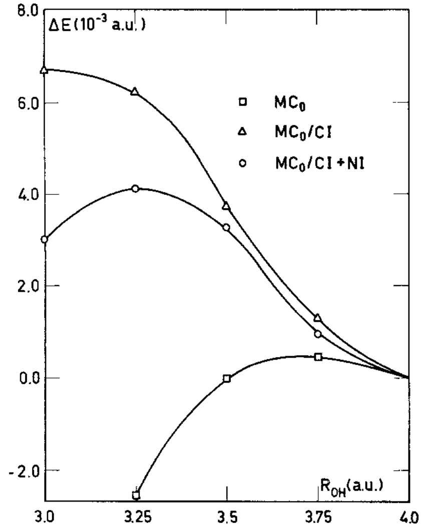

Fig. 4. Cross-section through the potential surface at fixed values of the parameters $\Theta = 104°$ and $R_{OO} = 2.212$ a.u. The zero of the energy scale is fixed to the point at $R_{OH} = 4.0$ a.u. for the three curves: squares refer to MC_0 calculations triangles to MC_0/CI and circles to $MC_0/CI+NI$ calculations

In a second step, the geometry of the activated complex was determined at the different levels of approximation by an optimization of the Θ and R_{OO} parameters at the R_{OH} distances determined in first step. The results of this optimization, derived from a coupled quadratic expression of the energy, are listed in Table 5 together with the resulting barrier height $E^{\neq}$. It can be seen that the barrier has disappeared at the MC_0 step. This conclusion is in agreement with the discussion presented in Sect 2.1 about the choice of the MC_0 configuration components. In fact together with a monotonic variation of the energy along the dissociation coordinate we observe as illustrated in Fig. 5, a parallel monotonic evolution of the 7a′ and 8a′ occupation numbers along this path.

Oppositely, the geometry optimization reduces but does not suppress the potential barrier at the MC_0/CI level of calculation. The same conclusion holds at the $MC_0/CI+NI$ level, leading to the final result of a barrier height of 0.19 eV. This value is in agreement with the GVB/CI result of D.W.G. and with the elaborate MC/CI result of M.B. The geometries found for the activated complex agree also with those obtained by these authors, except perhaps that a larger difference is observed for the R_{OH} distance.

Table 5. Potential barrier along the recombination path $O_2 + H \rightarrow HO_2$

					D.W.G.	
Parameter[a]	MC_0	MC_0/CI	$MC_0/CI+NI$	M.B.	POL-CI	GBV-CI
$E^{\neq}$	0.0	0.29	0.19	~0.1	~0.013	≤0.13
$\Theta^{\neq}$	—	126	125	~120	117.8	116
$R^{\neq}_{OO}$	—	2.28	2.28	2.33	2.33	2.33
$R^{\neq}_{OH}$	—	~3.0	3.25	3.76	4.0	3.3

[a] Barrier height in eV, angle Θ in degrees, distances in a.u.

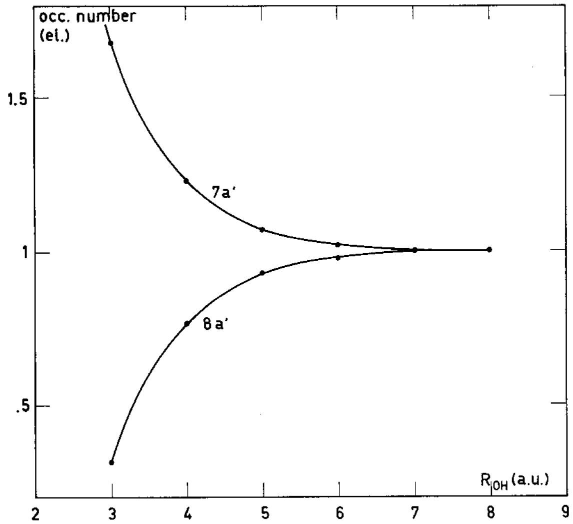

Fig. 5. Variation of the occupation numbers of the $7a'$ and $8a'$ orbitals in the MC_0(STO-3G) wavefunction along the R_{OH} dissociation coordinate in a cross-section through the potential surface ($R_{OO} = 2.212$ a.u. and $\Theta = 104°$)

Obviously, the presence of a potential barrier in our calculated hypersurface could result from a deficiency in the configuration expansion, as it was also possible for the previous calculations. However, the agreement encountered suggests that the eventual calculation artefacts are not amplified by using the economical method used here.

4. Conclusion

In this work we have applied an economical method developed recently for molecular correlation energy calculations to the determination of a potential energy surface. The $O_2 + H \rightarrow HO_2 \rightarrow OH + O$ system has proved to be an attractive system for his application. Indeed, it has been found that the shape of this hypersurface was very sensitive to the correlation effects. We have thus been interested in reproducing as accurately as possible the main parameters that characterize the topology of the surface, i.e. equilibrium geometries and vibrational frequencies of products, reactants and reaction intermediate, dissociation energies, energy gap between dissociation channels, geometry at the top of the hypothetical potential barrier and the corresponding activation energy. For each of these parameters, the changes in the calculated results with the progressive inclusion of the correlation energy has been discussed. The adjustment of basis set scale factors to ensure a balanced description of the different partners has also retained our attention.

The results have been found to be in good agreement with the available experimental data on the one hand and with the results proceeding from previous elaborate variational calculations on the other hand. The discrepancies are about 1° for the angles, ≤ 0.05 a.u. for the distances, 10% for the frequencies and within a range of 0.1 to 0.7 eV for the energy differences.

We think that such a method, more economical than purely variational approaches, gives reliable results and can provide an alternative way to calculate with useful accuracy potential energy surfaces.

Acknowledgments. This work is dedicated to the memory of Ph. Clercq who tragically left us. The authors thank Professor G. Verhaegen, for helpful discussions and for reading the manuscript and J. Breulet for the use of his non-internal correlation energy program. They are grateful to the Belgian "Ministère de la Politique Scientifique" and the "Fonds National de la Recherche Scientifique" for research grants (ARC 80–85/17 and FRFC 2.4552.82 respectively).

References

1. Glassman, I.: Combustion New-York: Academic 1977
2. Nicolet, M.: Etude des réactions chimiques de l'ozone dans la stratosphère. Institut Royal Météor. de Belgique
3. Liskow, D. H., Schaefer III, H. F., Bender, C. F.: J. Am. Chem. Soc. **93**, 6734 (1971); Gole, J. L., Hayes, E. F.: J. Chem. Phys. **57**, 360 (1972); Blint, R. J., Newton, M. D.: J. Chem. Phys. **59**, 6220 (1973)
4. Dunning, T. H. Jr., Walch, S. P., Goodgame, M. M.: J. Chem. Phys. **74**, 3482 (1981); Melius, C. F., Blint, R. J.: Chem. Phys. Letters. **64**, 183 (1979); Langhoff, S. R., Jaffe, R. L.: J. Chem. Phys. **71**, 2150 (1979)
5. Lievin, J., Breulet, J., Verhaegen, G.: Theoret. Chim Acta (Berl.) **60**, 339 (1981)
6. Breulet, J., Lievin, J.: Theoret. Chim. Acta (Berl.) **61**, 50 (1982)
7. Lievin, J., Breulet, J., Clercq, Ph., Metz, J.-Y.: Theoret. Chim. Acta (Berl.) **61**, 513 (1982)
8. Stevens, W. J., Das. G., Wahl, A. C., Krauss, M., Neuman, D.: J. Chem Phys. **61**, 3686 (1974)
9. Sinanoglu, O., Silverstone, H. J.: J. Chem. Phys. **44**, 1899 (1966)
10. Oksuz, I., Sinanoglu, O.: Phys. Rev. **53**, 735 (1969)
11. Verhaegen, G., Moser, C. M.: J. Phys. B.: Atom. Molec. Phys. **3**, 478 (1970); Desclaux, J. P., Moser, C. M., Verhaegen, G.: J. Phys. B.: Atom. Molec. Phys. **4**, 296 (1971)
12. Elbert, S. T., Cheung, L. M., Ruedenberg, K.: Nat. Resour. Comput. Chem. Software Cat., Vol. 1, prog. n°QM01 (ALIS), 1980
13. Whitten, J. L,. Hackmeyer, M.: J. Chem. Phys. **51**, 5584 (1969)
14. Hariharan, P. C., Pople, J. A.: Theoret. Chim. Acta (Berl.) **28**, 213 (1973)
15. Hehre, W. J., Ditchfiled, R., Pople, J. A.: J. Chem. Phys. **51**, 2657 (1969)
16. Hehre, W. J., Ditchfield, R., Pople, J. A.: J. Chem. Phys. **54**, 724 (1970)
17. Langhoff, S. R.: J. Chem. Phys. **61**, 1708 (1974)
18. Cade, P. E., Huo, W. M.: J. Chem Phys. **47**, 614 (1967)
19. Clementi, E., Roetti, C.: Atomic-data and nuclear-data tables **14**, 117 (1974)
20. Pulay, P., Meyer, W.: Mol. Phys. **27** (2), 473 (1973)
21. Huber, K. P., Herzberg, G.: Molecular spectra and molecular structure IV. Constants of diatomic molecules. New York: Van Nostrand Reinhold Company, (1979)
22. Turkett, R. P., Freedman, P. A., Jones, W. J.: Mol. Phys. **37**, 403 (1979)
23. JANAF Thermochemical Tables. Nat. Bur. Stand. (U.S.) **37**, (1971)

Received August 26, 1982